The Relaxation Spectrum for Gaussian Networks

A. Kloczkowski* and J. E. Mark

Department of Chemistry and Polymer Research Center, University of Cincinnati, Cincinnati, Ohio 45221

H. L. Frisch

Department of Chemistry, State University of New York at Albany, Albany, New York 12222

Received October 20, 1989; Revised Manuscript Received February 1, 1990

ABSTRACT: The relaxation spectrum has been calculated for treelike networks of phantom Gaussian chains subject to Rouse–Zimm dynamics. Our paper is an extension of earlier work by Graessley (*Macromolecules* **1980**, *13*, 372) by taking into account the bifunctional junctions dividing each chain between ϕ-functional junctions into n subchains of equal length, so that frictional interactions occur not only at multifunctional junctions but also at bifunctional ones. The relaxation spectrum and stress relaxation modulus have been calculated for varying number n of subchains. It has been found that bifunctional junctions considerably broaden the relaxation spectrum and give a more realistic description of the spectrum at shorter times.

Introduction

The dynamics of polymer chains in solution has been a subject of many papers since the pioneering work by Rouse.[1,2] Rouse assumed that a linear chain may be modeled as a collection of beads connected by subchains acting as springs. Such beads are subject to the stochastic Brownian forces and to the springlike forces from subchains directly connected to them. The hydrodynamic forces neglected originally by Rouse were included later by Zimm[2,3] for a better description of the chain dynamics. The theory has also been applied to ring, star, and comb-shaped molecules.[4-7] The Rouse–Zimm model successfully predicts the low-frequency relaxation behavior of chain molecules in all these cases.

A different kind of approach is the dynamic rotational isomeric state model,[8-10] which takes into account details of the molecular structure of the chain and accounts for the high-frequency relaxation behavior of polymers. The relaxation spectrum of a polymer network with the topology of the symmetrically grown tree in the low-frequency (hydrodynamic) limit has been studied by Chompff,[7] Doi,[11] and most completely Graessley.[12] A similar mathematical problem of the frequency spectrum for a system of mass points connected by springs with the topology of a Cayley tree was studied earlier by Rubin and Zwanzig.[13] In all these theories the network has been modeled as a collection of beads representing ϕ-functional junctions connected by phantomlike Gaussian chains acting as springs; i.e., the contribution of chains to the relaxation spectrum was neglected. This model applied to the treelike networks is not as successful as for small-chain molecules. The relaxation spectrum calculated for the treelike Gaussian networks by Graessley[12] is too narrow due to the simplified model of the structure of the network. Viscoelastic properties and distribution functions of perfect random networks have been studied by Martin and Eichinger[14,15] by calculating the eigenvalue spectra of Kirchhoff matrices[16] of random nets. The theoretical calculations of the density of eigenvalues of regular random graphs show[17] that the eigenvalue spectrum for an infinite, random graph effectively coincides with the spectrum for a tree graph. The dynamic structure factor for treelike networks has been studied by Ronca.[18]

In this paper we study the more realistic model of the network, taking into account the bifunctional junctions that divide chains joining ϕ-functional junctions into n subchains. For simplicity, we assume that all subchains have the same contour length and all junctions have the same functionality. We assume also that the network has the topology of the symmetrically grown tree, there are no loops or dangling chains in the network, and peripheral junctions are anchored to the fixed junctions, which do not fluctuate. We use the phantom network model; i.e., chains can move freely through one another and entanglement effects are not included. For simplicity, we assume that multifunctional and bifunctional junctions (beads) have the same frictional coefficient ζ.

Figure 1 shows an example of a micronetwork with $n = 4$ and $\phi = 4$ consisting of two tiers. The first tier consists of the central chain and the second tier of $2(\phi - 1)$ chains connected to the central chain. The third tier of the micronetwork would consist of $2(\phi - 1)^2$ chains directly connected with chains belonging to the second tier. Generally, the kth tier of the treelike network symmetrically grown around the central chain will consist of $2(\phi - 1)^{k-1}$ chains directly connected with $2(\phi - 1)^{k-2}$ chains of the $(k - 1)$th tier, and the kth-tiered micronetwork is built of all k tiers. It is assumed that peripheral junctions of the micronetwork are anchored to fixed junctions, which do not fluctuate. The micronetwork shown is symmetrically grown around the central chain and differs from the micronetwork symmetrically grown around the central junction studied by Graessley.[12] In the limit of infinite trees the difference between these networks vanishes. In the present paper we use Graessley's[12] method of separating the desired relaxation spectrum contributed by elements far removed from fixed points, because elements near fixed points give unrepresentative behavior.[13] We derive the general formula for the relaxation spectrum $H(\tau)$ and the stress relaxation modulus $G(t)$ as a function of $n - 1$ bifunctional junctions (n subchains) composing each chain. In the special case $n = 1$ we obtain Graessley's[12] results, as expected. We show that the inclusion of the bifunctional junctions in the model of polymer network broadens significantly the relaxation spectrum.

0024-9297/90/2223-3481$02.50/0

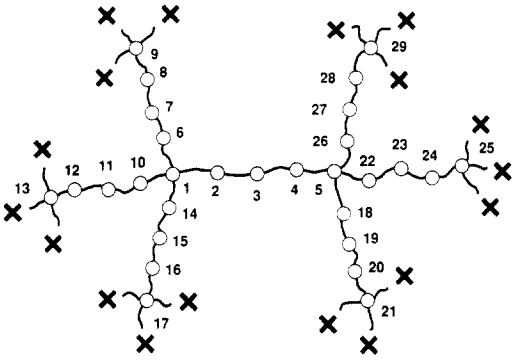

Figure 1. A symmetrically grown treelike micronetwork with functionality $\phi = 4$ and consisting of $J = 2$ tiers. Each chain comprises $n = 4$ subchains separated by $n - 1 = 3$ bifunctional junctions. The peripheral ϕ-functional junctions are anchored to fixed junctions, which do not fluctuate.

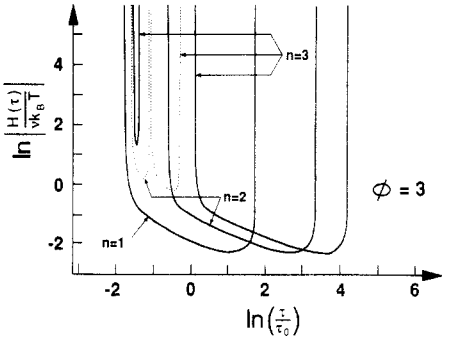

Figure 2. Relaxation spectra for trifunctional networks ($\phi = 3$) for different numbers n ($n = 1$–3) of subchains between ϕ-functional junctions. For $n = 1$ we obtain Graessley's spectrum.[12] Dotted lines correspond to negative $H(\tau)$.

Theory

Let $(\mathbf{R}_1, \mathbf{R}_2, ..., \mathbf{R}_N) = \{\mathbf{R}_n\}$ be the positions of beads (multifunctional and bifunctional junctions). The motion of each bead is determined by the force balance

$$\mathbf{F}_{drag} + \mathbf{F}_{spring} + \mathbf{F}_{stochastic} = 0 \tag{1}$$

which may be written

$$-\zeta\frac{d\{\mathbf{R}_n\}}{dt} - K\Gamma\{\mathbf{R}_n\} + \{\mathbf{f}_n\} = 0 \tag{2}$$

Here, ζ is the frictional coefficient, taken to be the same for each bead regardless of its functionality, K is the spring constant defined by

$$K = 3k_BT/\langle r^2\rangle_0 \tag{3}$$

where $\langle r^2\rangle_0$ is the mean square end-to-end distance for the unstretched subchain, k_B the Boltzmann constant, T the temperature, Γ the connectivity matrix, and $\{\mathbf{f}_n\}$ a set of random, stochastic forces acting on beads located at $\{\mathbf{R}_n\}$.

The connectivity matrix Γ, known also as the Kirchhoff matrix or valency–adjacency matrix[16] in graph theory, represents the topological structure of the system in a concise algebraic form. If beads i and j are directly connected by a spring, then the ijth element of matrix Γ is $\Gamma_{ij} = -1$; otherwise it is zero. The diagonal elements of Γ are equal to the sum of its nondiagonal elements in a given row (column) taken with the negative sign

$$\Gamma_{ii} = -\sum_j \Gamma_{ij} = -\sum_j \Gamma_{ji} \tag{4}$$

i.e., Γ_{ii} represents the functionality of the ith bead (junction).

The connectivity matrix Γ for a two-tiered micronetwork with $n = 4$ subchains between ϕ-functional junctions ($\phi = 4$) shown on Figure 1 is written below. The pattern of labeling of junctions enables one to write the connectivity matrix in a simple symmetrical form and to generalize it easily for larger trees.

$$\Gamma = \tag{5}$$

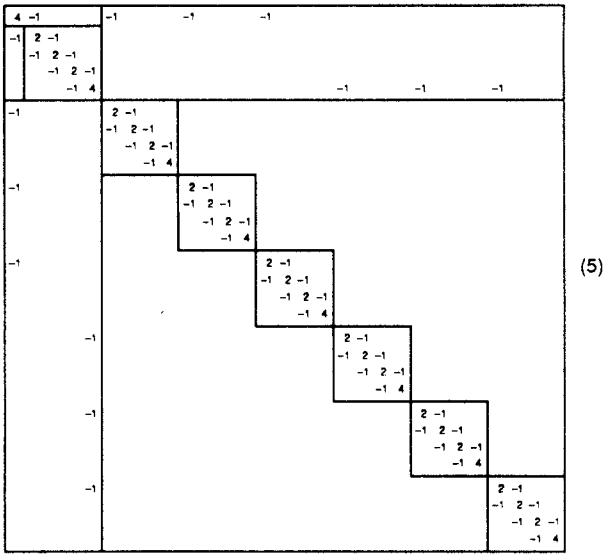

The matrix Γ might be partitioned into two square submatrices along the diagonal of Γ belonging to tier 1 (the central one) and tier 2. The entries 4 along the diagonal correspond to the multifunctional ($\phi = 4$) junctions, while the entries 2 refer to the bifunctional junctions along the chains. For simplicity, we assume that the peripheral junctions are ϕ-functional and each of them is anchored to $\phi - 1$ fixed junctions which do not fluctuate. Because of this assumption the submatrix corresponding to the last tier has the same structure as submatrices corresponding to inner tiers.

We might easily generalize the connectivity matrix Γ to the case of a J-tiered network consisting of ϕ-functional junctions joined by n equal length subchains (i.e., separated by $n - 1$ bifunctional junctions). The dimension of the matrix Γ is $N \times N$, where

$$N = 2n\frac{(\phi - 1)^J - 1}{\phi - 2} - n + 1 \tag{6}$$

The matrix Γ might also be partitioned into square submatrices corresponding to subsequent tiers. The dimension of the first submatrix corresponding to the central first tier is $N_1 \times N_1$ with

$$N_1 = n + 1 \tag{7}$$

and that of the second submatrix is $N_2 \times N_2$ with

$$N_2 = 2n(\phi - 1) \tag{8}$$

Generally, the dimension of the square submatrix corresponding to the jth tier is $N_j \times N_j$ with

$$N_j = 2n(\phi - 1)^{j-1} \tag{9}$$

for $2 \le j \le J$. In each of these submatrices we can isolate along the diagonal the sub-submatrices $\mathbf{A}_n$ of order $n \times n$ corresponding to a given ϕ-functional junction within a given tier. Each of these sub-submatrices has the form

$\mathbf{A}_n =$

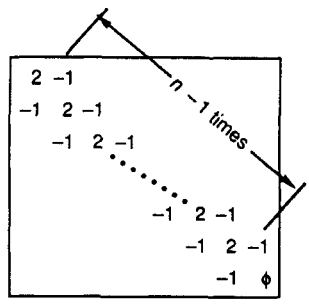

(10)

The eigenvalues λ_i (i = 1, 2, ..., N) of the connectivity-matrix $\mathbf{\Gamma}$ are solutions of the characteristic (secular) equation

$$\det(\mathbf{\Gamma} - \lambda\mathbf{I}_N) = 0 \tag{11}$$

where $\mathbf{I}_N$ is the identity matrix of order N.

Each eigenvalue λ_i is associated with the relaxation time of the ith mode

$$\tau_i = \tau_0/\lambda_i \qquad i = 1, 2, ..., N \tag{12}$$

Here, τ_0 is the primary relaxation time of a single unattached subchain

$$\tau_0 = \zeta/K \tag{13}$$

determined by the frictional coefficient ζ of the beads and the spring constant K (given by eq 3) of a subchain. For a very large system in the limit $N \to \infty$, the distribution of eigenvalues $\lambda(\xi)$ and relaxation times $\tau(\xi)$ is described by the continuous variable ξ, and the relaxation spectrum $H(\tau)$ is defined by

$$H(\tau) = -\nu k_B T \frac{d\xi}{d \ln \tau} \tag{14}$$

where ν is the number of beads per unit volume. The relaxation modulus $G(t)$ is defined as an integral of the relaxation spectrum $H(\tau)$

$$G(t) = G_e + \int_{-\infty}^{\infty} H(\tau) e^{-t/\tau} d \ln \tau \tag{15}$$

or alternatively

$$G(t) = G_e + \nu k_B T \sum_{i=1}^{N} \exp\left(-\frac{\lambda_i t}{\tau_0}\right) \tag{16}$$

where G_e is the equilibrium shear modulus of the network. The main problem in calculating the relaxation spectrum $H(\tau)$ and relaxation modulus $G(t)$ is to solve the eigenvalue problem, i.e., eq 11. To calculate the determinant $\det(\mathbf{\Gamma} - \lambda\mathbf{I}_N)$, we eliminate all nonzero, nondiagonal elements in the upper right half of the matrix $\mathbf{\Gamma} - \lambda\mathbf{I}_N$. This method has been previously used by some of us[19] for the calculation of the inverse matrix $\mathbf{\Gamma}^{-1}$. We start from the square submatrix corresponding to the last Jth tier. It contains

$$m_J = 2(\phi - 1)^{J-1} \tag{17}$$

square sub-submatrices $\mathbf{A}_n - \lambda\mathbf{I}_n$ of order $n \times n$ along the diagonal.

We divide the last nth row of the matrix $\mathbf{A}_n - \lambda\mathbf{I}_n$ by $\phi - \lambda$ and add it to the preceding $(n-1)$th row. It changes the $(n-1)$th diagonal element from $2 - \lambda$ to

$$\frac{(\phi - \lambda)(2 - \lambda) - 1}{\phi - \lambda} \tag{18}$$

Next we divide the $(n-1)$th row by the expression in eq 18 and add it to the $(n-2)$th row. By doing this, we change the $(n-2)$th diagonal element of $\mathbf{A}_n - \lambda\mathbf{I}_n$ from $2 - \lambda$ to

$$\frac{(\phi - \lambda)[(2 - \lambda)^2 - 1] - (2 - \lambda)}{(\phi - \lambda)(2 - \lambda) - 1} \tag{19}$$

The continuation of this process finally leads to

$$\frac{(\phi - \lambda)U_{n-1}(x) - U_{n-2}(x)}{(\phi - \lambda)U_{n-2}(x) - U_{n-3}(x)} \tag{20}$$

as the first diagonal element of the $\mathbf{A}_n - \lambda\mathbf{I}_n$ matrix. Here, $U_n(x)$ is the Chebyshev polynomial of the second kind[20,21] of the variable

$$x = 1 - \lambda/2 \tag{21}$$

The determinant of the $\mathbf{A}_n - \lambda\mathbf{I}_n$ matrix is

$$\det(\mathbf{A}_n - \lambda\mathbf{I}_n) = (\phi - \lambda)U_{n-1}(x) - U_{n-2}(x) \tag{22}$$

since the determinant of the semidiagonalized matrix is equal to the product of elements along the diagonal. Using the known recursion formula for Chebyshev polynomials,[20,21] we may write eq 22 as

$$\det(\mathbf{A}_n - \lambda\mathbf{I}_n) = U_n(x) + (\phi - 2)U_{n-1}(x) \tag{23}$$

with x given by eq 21.

There are m_J $n \times n$ dimensional sub-submatrices $\mathbf{A}_n$ along the diagonal of the submatrix $\mathbf{\Gamma}_J$ corresponding to the last Jth tier (see eq 17). Therefore, the determinant of the submatrix $\mathbf{\Gamma}_J - \lambda\mathbf{I}_{N_J}$ is

$$\det(\mathbf{\Gamma}_J - \lambda\mathbf{I}_{N_J}) = [U_n(x) + (\phi - 2)U_{n-1}(x)]^{m_J} \tag{24}$$

Here, $\mathbf{I}_{N_J}$ is the identity matrix of order N_J given by eq 9.

To eliminate the entries -1 of the matrix $\mathbf{\Gamma} - \lambda\mathbf{I}_N$ which correspond to the connectivity between elements of the last Jth tier and the $(J-1)$th tier, we change the diagonal elements of the $(J-1)$th tier in rows containing these -1s from

$$a_1 = \phi - \lambda \tag{25}$$

to

$$a_2 = \phi - \lambda - \frac{(\phi - 1)[a_1 U_{n-2}(x) - U_{n-3}(x)]}{a_1 U_{n-1}(x) - U_{n-2}(x)} \tag{26}$$

because there are $\phi - 1$ such entries (-1s) in each row containing element a_1, on the right side of a_1. This makes possible the diagonalization of the sub-submatrices $\mathbf{A}_n - \lambda\mathbf{I}_n$ corresponding to the $(J-1)$th tier (now $\mathbf{A}_n - \lambda\mathbf{I}_n$ is different from the result shown in eq 10 since its lowest diagonal element equals a_2 instead of $a_1 = \phi - \lambda$) and this leads to

$$\det(\mathbf{A}_n - \lambda\mathbf{I}_n) = a_2 U_{n-1}(x) - U_{n-2}(x) \tag{27}$$

with a_2 given by eq 26 and x by eq 21.

There are m_{J-1} such sub-submatrices along the diagonal of the submatrix $\mathbf{\Gamma}_{J-1} - \lambda\mathbf{I}_{N_{J-1}}$ corresponding to the $(J-1)$th tier, and its determinant becomes

$$\det(\mathbf{\Gamma}_{J-1} - \lambda\mathbf{I}_{N_{J-1}}) = [a_2 U_{n-1}(x) - U_{n-2}(x)]^{m_{J-1}} \tag{28}$$

with m_{J-1} given by eq 17.

Generally, the determinant for the jth submatrix $\mathbf{\Gamma}_j - \lambda\mathbf{I}_{N_j}$ corresponding to the jth tier ($j = J, J-1, ..., 3, 2$) is

$$\det(\mathbf{\Gamma}_j - \lambda\mathbf{I}_{N_j}) = [a_{J-j+1} U_{n-1}(x) - U_{n-2}(x)]^{m_j} \tag{29}$$

where the coefficients a_k satisfy the recurrence relation

$$a_k = \phi - \lambda - \frac{(\phi - 1)[a_{k-1}U_{n-2}(x) - U_{n-3}(x)]}{a_{k-1}U_{n-1}(x) - U_{n-2}(x)} \quad (30)$$

for $2 \le k \le J$, with a_1 given by eq 25 and m_j ($2 \le j \le J$) by eq 17. One should note that the method of enumerating coefficients a_k is inverse to the counting of the tiers. The last Jth peripheral tier anchored to the fixed junctions is associated with the coefficient a_1, while the first (central) tier is associated with the coefficient a_J.

Equation 28 gives determinants of all submatrices $\Gamma_j - \lambda \mathbf{I}_{N_j}$ ($2 \le j \le J$) except for the first tier ($j = 1$). The determinant of $\Gamma_1 - \lambda \mathbf{I}_{N_1}$ corresponding to the first tier is

$$\det \Gamma_1 - \lambda \mathbf{I}_{N_1} = \begin{bmatrix} a_J & -1 & & & \\ -1 & 2-\lambda & -1 & & \\ & \ddots & \ddots & \ddots & \\ & & -1 & 2-\lambda & -1 \\ & & & -1 & a_J \end{bmatrix} = a_J^2 U_{n-1}(x) - 2a_J U_{n-2}(x) + U_{n-3}(x) \quad (31)$$

with coefficient a_J given by recurrence relation 30.

The characteristic eq 11 for eigenvalues of the connectivity matrix Γ is given by the product of determinants $\det(\Gamma_j - \lambda \mathbf{I}_{N_j})$ of submatrices Γ_j corresponding to subsequent tiers ($1 \le j \le J$)

$$\det(\Gamma - \lambda \mathbf{I}_N) = \prod_{j=1}^{J} \det(\Gamma_j - \lambda \mathbf{I}_{N_j}) = [a_1 U_{n-1}(x) - U_{n-2}(x)]^{m_J}[a_2 U_{n-1}(x) - U_{n-2}(x)]^{m_{J-1}} \times \ldots \times [a_{J-1}U_{n-1}(x) - U_{n-2}(x)]^{m_2} \times \{a_J^2 U_{n-1}(x) - 2a_J U_{n-2}(x) + U_{n-3}(x)\} = 0 \quad (32)$$

The coefficients a_j ($1 \le j \le J$) are given by eq 30 and exponents m_j ($2 \le j \le J$) by eq 17. In the special case when there are no bifunctional junctions ($n = 1$), we recover eq 15 of Graessley.[12]

Introducing the compact notation

$$A_k = a_k U_{n-1}(x) - U_{n-2}(x) \qquad 1 \le k \le J \quad (33)$$

the characteristic equation for the connectivity matrix Γ (eq 32) might be written

$$\det(\Gamma - \lambda \mathbf{I}_N) = A_1^{m_J} A_2^{m_{J-1}} \times \ldots \times A_{J-1}^{m_2}(A_J^2 - 1) = 0 \quad (34)$$

We used a known relation for Chebyshev polynomials[21]

$$U_{n-2}^2(x) - U_{n-1}(x)U_{n-3}(x) = 1 \quad (35)$$

calculating the term corresponding to the first tier. Equation 34 has N (see eq 6) λ roots, each root representing an eigenvalue associated with a specific mode. A relatively small number ($2nJ$) of these roots are the solutions of the equation

$$A_J^2 - 1 = 0 \quad (36)$$

The remaining number

$$2n\left[\frac{(\phi - 1)^J - 1}{\phi - 2} - J\right] - n + 1 \quad (37)$$

of roots represent the solutions of the equation

$$A_k = 0 \quad (38)$$

for $1 \le k \le J - 1$.

The coefficients A_k are complicated functions of λ and ϕ, as are the a_k. From eq 30, the recursion formula for Chebyshev polynomials, and the definition (33), there follows the recurrence relation for coefficients A_k:

$$A_1 = U_n(x) + (\phi - 2)U_{n-1}(x) \quad (39)$$

and

$$A_k = U_n(x) + (\phi - 2)U_{n-1}(x) - (\phi - 1)U_{n-2}(x) - \frac{\phi - 1}{A_{k-1}} \quad (40)$$

with $2 \le k \le J$.

The detailed solution of this recurrence relation is shown in Appendix A. The result is

$$A_k = \sqrt{\phi - 1}\,\frac{U_k(y) + \sqrt{\phi - 1}\,U_{n-2}(x)U_{k-1}(y)}{U_{k-1}(y) + \sqrt{\phi - 1}\,U_{n-2}(x)U_{k-2}(y)} \qquad 1 \le k \le J \quad (41)$$

with

$$y = \frac{U_n(x) + (\phi - 2)U_{n-1}(x) - (\phi - 1)U_{n-2}(x)}{2\sqrt{\phi - 1}} \quad (42)$$

and with x given by eq 21.

Equation 38 for the eigenvalues reads

$$U_k\left[\frac{U_n\left(1 - \frac{\lambda}{2}\right) + (\phi - 2)U_{n-1}\left(1 - \frac{\lambda}{2}\right) - (\phi - 1)U_{n-2}\left(1 - \frac{\lambda}{2}\right)}{2\sqrt{\phi - 1}}\right] + \sqrt{\phi - 1}\,U_{n-2}\left(1 - \frac{\lambda}{2}\right) \times U_{k-1}\left[\frac{U_n\left(1 - \frac{\lambda}{2}\right) + (\phi - 2)U_{n-1}\left(1 - \frac{\lambda}{2}\right) - (\phi - 1)U_{n-2}\left(1 - \frac{\lambda}{2}\right)}{2\sqrt{\phi - 1}}\right] = 0 \quad (43)$$

for $1 \le k \le J - 1$.

This highly complicated double Chebyshev polynomial expression is the solution of our problem. The λ dependence in eq 43 is shown explicitly. Equation 43 is a polynomial of order kn in λ. The kn λ roots of eq 43 give eigenvalues of the connectivity matrix Γ associated with the $(J - k + 1)$th tier. For the special case when $n = 1$, i.e., when there are no bifunctional junctions, eq 43 reduces to

$$U_k\left(\frac{\phi - \lambda}{2\sqrt{\phi - 1}}\right) = 0 \quad (44)$$

and since zeroes of the Chebyshev polynomial $U_k(x)$ are

$$x_r = \cos\frac{\pi r}{k + 1} \qquad r = 1, 2, \ldots, k \quad (45)$$

we immediately obtain Graessley's result[12]

$$\lambda_r = \phi - 2\sqrt{\phi - 1}\cos\frac{\pi r}{k + 1} \qquad r = 1, 2, \ldots, k \quad (46)$$

For a linear chain, $\phi = 2$, using the trigonometric representation for Chebyshev polynomials,[21] one can show that eq 43 is equivalent to

$$U_{kn}\left(1 - \frac{\lambda}{2}\right) = 0 \quad (47)$$

For a tree with functionality $\phi = 2$ the number of chains in each tier is $m_j = 2$ ($1 \le j \le J$) and the most important becomes the term (eq 31) corresponding to the first (central) tier. Equation 36 associated with the first tier for $\phi = 2$ becomes

$$U_{(2J-1)n+1}\left(1 - \frac{\lambda}{2}\right) = 0 \quad (48)$$

The 2-functional tree of J tiers has

$$N = (2J-1)n \tag{49}$$

subchains and the result (eq 48) is the same as for the Rouse chain of length N (N springs) with ends attached to fixed points.

We have not been able to solve eq 43 analytically for $\phi > 2$ and $n > 1$. The eigenvalues for small micronetworks can be obtained by the numerical solution of eq 43, which means finding roots of the polynomial of degree kn with $1 \le k \le J-1$.

The eigenvalues associated with the first tier (i.e., for $k = J$) are obtained from the numerical solution of eq 36 or by writing explicitly

$$\left[\frac{U_k(y) + \sqrt{\phi-1}U_{n-1}(x)U_{k-1}(y)}{U_{k-1}(y) + \sqrt{\phi-1}U_{n-1}(x)U_{k-2}(y)}\right]^2 = \frac{1}{\phi-1} \tag{50}$$

with x and y given by eqs 21 and 42, respectively. For large networks consisting of many tiers this method cannot be used. Instead, we are looking for the asymptotic analytical solution of the model for a very large network in the limit when the number of tiers J goes to infinity. Following Graessley[12] we consider only junctions that are far removed from fixed points, because elements near fixed points show unrepresentative behavior.[13]

Such a separation procedure seems physically justifiable and enables us to obtain a continuous spectrum,[12] while retaining all elements of the network gives an unusual, discontinuous spectrum.[13] If the fixed points are located near the polymer's surface, our assumption means that we are interested in the relaxation spectrum from the bulk of the polymer, unperturbed by surface effects. We have shown in Appendix B that in the limit $k \to \infty$, for tiers far removed from the surface, the asymptotic analytical solution of eqs 43 and 50 is

$$U_n\left(1-\frac{\lambda}{2}\right) + (\phi-2)U_{n-1}\left(1-\frac{\lambda}{2}\right) - (\phi-1)U_{n-2}\left(1-\frac{\lambda}{2}\right) = 2\sqrt{\phi-1}\cos\frac{\pi r}{k+1} \tag{51}$$

with $r = 1, 2, ..., k$. Equation 51 represents the simplified analytical solution of the eigenvalue problem for the network. Instead of a polynomial of order nk in λ (eq 43), we obtained a set of k polynomial equations of order n. The λ roots of eq 51 might be easily obtained for $n = 1$ and $n = 2$ only. For $n = 1$, when there are no bifunctional junctions in the network model, we recover Graessley's solution,[12] given by eq 46. The solution of eq 51 for $n = 2$, when there is one bifunctional junction between ϕ-functional ones, is

$$\lambda_{r,1} = \frac{2 + \phi + \sqrt{\phi^2 + 4 + 8\sqrt{\phi-1}\cos\frac{\pi r}{k+1}}}{2} \tag{52}$$

and

$$\lambda_{r,2} = \frac{2 + \phi - \sqrt{\phi^2 + 4 + 8\sqrt{\phi-1}\cos\frac{\pi r}{k+1}}}{2} \tag{53}$$

with $r = 1, 2, ..., k$. The expression

$$\phi^2 + 4 + 8\sqrt{\phi-1}\cos\frac{\pi r}{k+1} \tag{54}$$

is always nonnegative and might be zero only for $\phi = 2$. For larger n eq 51 might be solved numerically. The relaxation spectrum $H(\tau)$, however, might be obtained without numerical solution of eq 51. It is defined by eq 14.

A continuous parameter ξ (in the limit $k \to \infty$) describing the relaxation times associated with the $(J-k+1)$th tier far removed from fixed junctions is

$$\xi = \frac{r}{k+1} \qquad r = 1, 2, ..., k \qquad \text{i.e. } 0 < \xi < 1 \tag{55}$$

The relaxation time corresponding to the rth mode is

$$\tau(r) = \lim_{k\to\infty}\frac{\tau_0}{\lambda_r} \tag{56}$$

where the primary relaxation time τ_0 of a single, free subchain is given by eq 13. From eqs 51 and 55 it follows that

$$\xi = \frac{1}{\pi}\arccos\left[\frac{U_n(x) + (\phi-2)U_{n-1}(x) - (\phi-1)U_{n-2}(x)}{2\sqrt{\phi-1}}\right] \tag{57}$$

with x given by eq 21, and then

$$\frac{d\xi}{d\lambda} = -\frac{1}{2}\frac{d\xi}{dx} = \frac{1}{2\pi} \times \frac{U'_n(x) + (\phi-2)U'_{n-1}(x) - (\phi-1)U'_{n-2}(x)}{\sqrt{4(\phi-1) - [U_n(x) + (\phi-2)U_{n-1}(x) - (\phi-1)U_{n-2}(x)]^2}} \tag{58}$$

where[21]

$$U'_n(x) \equiv \frac{d}{dx}U_n(x) = \frac{1}{x^2-1}[(n+2)T_{n+1}(x) - U_{n+1}(x)] \tag{59}$$

and the relaxation spectrum $H(\tau)$ becomes

$$H(\tau) = \frac{\nu k_B T \tau_0}{2\pi\tau} \times \frac{[U'_n(x) + (\phi-2)U'_{n-1}(x) - (\phi-1)U'_{n-2}(x)]}{\sqrt{4(\phi-1) - [U_n(x) + (\phi-2)U_{n-1}(x) - (\phi-1)U_{n-2}(x)]^2}} \tag{60}$$

with

$$x = 1 - \frac{\lambda}{2} = 1 - \frac{\tau_0}{2\tau} \tag{61}$$

In the case $n = 1$, when there are no bifunctional junctions between the ϕ-functional ones, we have

$$H(\tau) = \frac{\nu k_B T}{2\pi\sqrt{\phi-1}}\frac{\tau_0}{\tau}\frac{1}{\left[1 - \frac{(\phi - \tau_0/\tau)^2}{4(\phi-1)}\right]^{1/2}} \tag{62}$$

i.e., we obtain the same result as Graessley. (τ_0^G in Graessley's paper is differently defined: $\tau_0^G = \tau_0/\phi$.)

The relaxation spectrum $H(\tau)$ given by eq 60 is real for relaxation times τ satisfying the inequality

$$-2\sqrt{\phi-1} < U_n(x) + (\phi-2)U_{n-1}(x) - (\phi-1)U_{n-2}(x) < 2\sqrt{\phi-1} \tag{63}$$

with the τ dependence of x given by eq 61. In the case $n = 1$ studied by Graessley,[12] this means

$$\tau_{min} = \frac{\tau_0}{\phi + 2\sqrt{\phi-1}} < \tau < \tau_{max} = \frac{\tau_0}{\phi - 2\sqrt{\phi-1}} \tag{64}$$

and there is one continuous band of relaxation times defined by eq 64. For $n = 2$, when there is one bifunctional junction dividing each chain into two subchains in the model of the network, we have two separate (nonover-

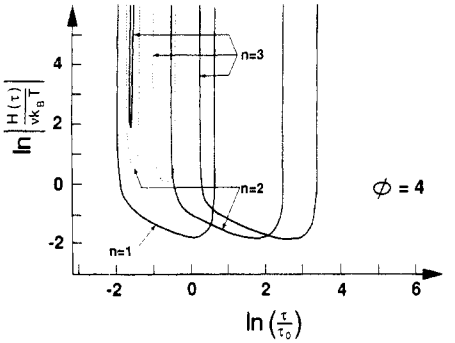

Figure 3. Relaxation spectra for tetrafunctional networks ($\phi = 4$); see legend to Figure 3.

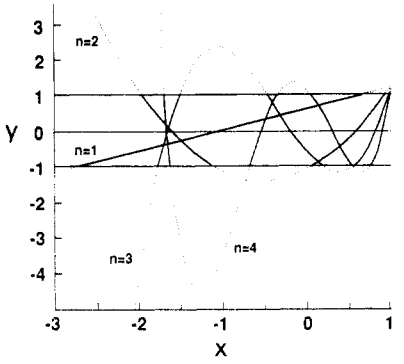

Figure 4. Plot of the function $y(x) = [U_n(x) + (\phi - 2)U_{n-1}(x) - (\phi - 1)U_{n-2}(x)]/[2\sqrt{\phi - 1}]$ for a tetrafunctional network for varying number n (n = 1–4) of subchains between ϕ-functional junctions. The infinite relaxation time corresponds to $x = 1$. For each n, the bands in the relaxation spectrum are determined by the inequality $-1 < y < 1$. Only the bands with positive slopes of $y(x)$ are physical.

lapping) bands (see eqs 52 and 53)

$$\tau_{\min,1} = \frac{2\tau_0}{2 + \phi + \sqrt{\phi^2 + 4 + 8\sqrt{\phi - 1}}} < \tau_1 < \tau_{\max,1} = \frac{2\tau_0}{2 + \phi + \sqrt{\phi^2 + 4 - 8\sqrt{\phi - 1}}} \quad (65)$$

$$\tau_{\min,2} = \frac{2\tau_0}{2 + \phi - \sqrt{\phi^2 + 4 - 8\sqrt{\phi - 1}}} < \tau_2 < \tau_{\max,2} = \frac{2\tau_0}{2 + \phi - \sqrt{\phi^2 + 4 + 8\sqrt{\phi - 1}}} \quad (66)$$

The first band τ_1 is unphysical as shown below. The larger n, the more bands we have and the resulting spectrum becomes highly complex.

The numerator of eq 60, containing derivatives of Chebyshev polynomials, might become negative for larger n, leading to some negative parts of the spectrum $H(\tau)$, which are unphysical. Figures 2 and 3 show relaxation spectra for trifunctional (Figure 2) and tetrafunctional (Figure 3) networks with varying number n of bifunctional junctions included in the model. For convenience, Figures 2 and 3 are plotted on a logarithmic scale. Since $H(\tau)$ might be negative, we plotted $\ln|H(\tau)/\nu k_B T|$, with dotted lines corresponding to negative $H(\tau)$. The negative $H(\tau)$ is related to bands with negative slope of $y(x)$ vs x, as might be seen from Figure 4. This part of the spectrum is unphysical and should be ignored. The source of this peculiarity is probably the mathematical approximations used in treating the model. The unphysical, negative parts of the spectrum occur in the high-frequency region of the spectrum, for which the separation procedure proposed by Graessley[12] may be questionable. However, the most important and physically significant result is the low-frequency part of the spectrum corresponding to relaxation times τ greater than the primary relaxation time τ_0. It is interesting that the central part of this band is almost linear with slope $-1/2$. The inclusion of the bifunctional junctions in the model of the network broadens the spectrum considerably.

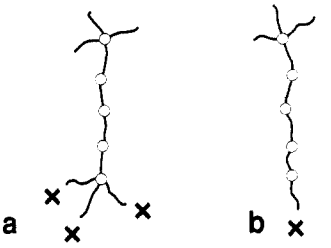

Figure 5. Two different possibilities for anchoring peripheral junctions: (a) the functionality ϕ of a peripheral junction is preserved; (b) the peripheral junction is anchored to only one fixed junction.

Knowledge of all the eigenvalues enables us to calculate the relaxation modulus $G(t)$ for the micronetwork by using eq 16. Equation 32 for all eigenvalues might be written with the help of the A_k's (see eq 33) as

$$\det(\Gamma - \lambda \mathbf{I}_N) = A_1^{m_J} A_2^{m_{J-1}} \ldots A_{J-1}^{m_2}(A_J^2 - 1)\frac{1}{U_{n-1}(x)} = 0 \quad (67)$$

where m_j ($1 \le j \le J$) is given by eq 17. The coefficients A_k satisfy eq 41; i.e.

$$A_k = \sqrt{\phi - 1}\frac{U_k(y) + \sqrt{\phi - 1}U_{n-2}(x)U_{k-1}(y)}{U_{k-1}(y) + \sqrt{\phi - 1}U_{n-2}(x)U_{k-2}(y)} \equiv \sqrt{\phi - 1}\frac{S_k}{S_{k-1}} \quad (68)$$

for $1 \le k \le J$, and eq 67 becomes

$$\det(\Gamma - \lambda \mathbf{I}_N) = (\phi - 1)^M\left[\prod_{j=1}^{J-1} S_j^{2(\phi-2)(\phi-1)^{J-1-j}}\right] \times \left(S_J^2 - \frac{1}{\phi - 1}S_J^2\right)\frac{1}{U_{n-1}(x)} \quad (69)$$

with

$$M = \frac{1}{2}\sum_{j=1}^{J} m_j = \frac{(\phi - 1)^J - 1}{\phi - 2} \quad (70)$$

If $\lambda_k(r)$ denotes the rth root ($1 \le r \le kn$) of the equation $S_k = 0$ (eq 43) for $1 \le k \le J - 1$ and $\lambda_J(r)$ ($1 \le r \le 2Jn$) roots of eq 50, then the relaxation modulus $G(t)$ is

$$G(t) = G_e + \nu k_B T\left\{\sum_{r=1}^{2nJ}\exp\left[-\frac{t\lambda_J(r)}{\tau_0}\right] + 2(\phi - 2)\sum_{k=1}^{J-1}(\phi - 1)^{J-1-k}\sum_{r=1}^{kn}\exp\left[-\frac{t\lambda_k(r)}{\tau_0}\right]\right\} \quad (71)$$

where G_e is the equilibrium shear modulus of the network. Equations 69 and 71 differ from the corresponding equations in Graessley's paper[12] due to the difference in the trees. Specifically, we study trees symmetrically grown around a central chain, while Graessley studied trees grown around a central junction. In the limit of infinite trees the difference between these types of trees disappears. For large networks ($J \gg 1$) the double sum in eq 71 is dominant. Equation 71 shows that elements

Table I
Calculated Maximum Relaxation Times[a]

n	τ_{max}/τ_0	τ_{max}^{appr}/τ_0
1	1.87	1.87
2	11.0	11.2
3	27.5	28.0
4	51.4	52.2
5	82.3	84.0
7	166	170
10	349	355

[a] Maximum relaxation times τ_{max} for a tetrafunctional Gaussian network having different numbers n of subchains between multifunctional junctions, as obtained by numerical solution of eq 63, and relaxation times τ_{max}^{appr}, as calculated from eq 80. Both quantities are normalized by the primary relaxation time τ_0.

of the network close to fixed junctions (corresponding to small k) might give important contributions to relaxation modulus because of the power dependence of $(\phi - 1)$ in eq 71.

Using the separation method to calculate the relaxation spectrum $H(\tau)$ given by eq 60, we neglect the contribution from these elements to the relaxation modulus. However, the long relaxation times (small eigenvalues) which mainly determine the relaxation modulus are associated with elements of the network far from fixed junctions and this might justify the separation method we used. Applying eq 16 with $\lambda(r)$ determined by eq 51 to calculate the relaxation spectrum for $n = 1$, we obtain Graessley's result

$$G(t) = G_e + \nu k_B T e^{-\phi t/\tau_0} I_0(2\sqrt{\phi - 1}(t/\tau_0)) \quad (72)$$

Generally, for any n we have

$$G(t) = G_e + \frac{\nu k_B T}{\pi} e^{-2t/\tau_0} \int_{-\infty}^{1} dx \frac{e^{2tx/\tau_0}[U'_n(x) + (\phi - 2)U'_{n-1}(x) - (\phi - 1)U'_{n-2}(x)]}{\sqrt{4(\phi - 1) - [U_n(x) + (\phi - 2)U_{n-1}(x) - (\phi - 1)U_{n-2}(x)]^2}} \quad (73)$$

where the integral is defined only for bands $|y| < 1$ with positive slopes of $y(x)$, with y given by eq 42; otherwise, it is zero.

Discussion

The inclusion of the bifunctional junctions in the network model broadens the relaxation spectrum considerably. If there are no bifunctional junctions ($n = 1$), the maximum relaxation time is

$$\tau_{max} = \frac{\tau_0}{\phi - 2\sqrt{\phi - 1}} \quad (74)$$

Thus, even in the most extreme case of trifunctional junctions, $\tau_{max} \cong 5.83\tau_0$. As the functionality of the network increases, the maximum relaxation time decreases. For functionality $\phi > 5$ the maximum relaxation time τ_{max} becomes even lower than the primary relaxation time τ_0. The additional bifunctional junctions acting as frictional beads improve the relaxation spectrum considerably. Table I shows the ratio τ_{max}/τ_0 of maximum relaxation time to the primary relaxation time for the tetrafunctional network ($\phi = 4$) as a function of number of subchains n (separated by $n - 1$ bifunctional junctions) between multifunctional junctions. The maximum relaxation time increases rapidly as n grows. The additional characteristic feature of our model is the multiband structure of the relaxation spectrum. The bands are determined by the inequality 63; i.e., by $|y| < 1$, with y defined by eq 42.

Figure 4 shows the dependence of y with respect to x for a tetrafunctional network for a different number n of subchains in the model. Only bands with positive slopes of $y(x)$ vs x are physical. The relaxation time is related to x through eq 61; i.e.

$$\tau = \frac{\tau_0}{2(1 - x)} \quad (75)$$

The plots in Figure 4 have been done only for $x < 1$, since $x > 1$ corresponds to unphysical, negative relaxation times. For a given n each band corresponds to a part of the $y(x)$ plot satisfying the inequality 63. For n subchains in the model network we have n bands in the spectrum. Only half of these bands are physical; bands with negative slopes of $y(x)$, which give negative $H(\tau)$, are unphysical. The most important, low-frequency part of the spectrum for relaxation times $\tau_0 < \tau < \infty$ corresponds to $1/2 < x < 1$. The point $x = 1$ corresponds to an infinite relaxation time.

Since for $x = 1$

$$y(1) = \frac{\phi}{2\sqrt{\phi - 1}} \quad (76)$$

is independent of n, all curves in Figure 4 coincide at this point. Additionally, since $y(1)$ (given by eq 76) is always greater than 1 regardless of the functionality ϕ of the network ($\phi > 2$), there is always a finite maximum relaxation time τ_{max} for the network. The distance Δy between points $y(1)$ and $y = 1$ for $x = 1$ in Figure 4

$$\Delta y = y(1) - 1 = \frac{\phi}{2\sqrt{\phi - 1}} - 1 \quad (77)$$

is relatively small; e.g., $\Delta y = 0.061$ for a trifunctional network and $\Delta y = 0.155$ for a tetrafunctional one. We might approximate the curves in Figure 4 for x in the vicinity of $x = 1$ by straight lines passing through the point $(x, y) = (1, 1)$ with slopes determined by derivatives $y'(1)$. This approximation enables us to calculate the maximum relaxation time

$$\tau_{max}^{appr} \cong \frac{\tau_0}{2} \frac{y'(1)}{\Delta y} \quad (78)$$

Using eq 42 and the relation

$$\lim_{x \to 1} \frac{d}{dx} U_n(x) = \frac{1}{3} n(n + 1)(n + 2) \quad (79)$$

for Chebyshev polynomials, we may write eq 78 as

$$\tau_{max}^{appr} = \tau_0 \frac{n(n\phi - \phi + 2)}{2(\phi - 2\sqrt{\phi - 1})} \quad (80)$$

There is very good agreement between the approximate relaxation times τ_{max}^{appr} calculated from eq 80 and those obtained numerically from eq 63 as exact maximum relaxation times. This is shown in Table I. The approximate solution overestimates the maximum relaxation time (except for $n = 1$) due to the positive curvature of $y(x)$ at $x = 1$. Using the second-order Taylor expansion might additionally improve the results. Equation 80 shows that for very large n the maximum relaxation time goes as the square of n:

$$\tau_{max} \approx \tau_1 \phi n^2/2 \quad (81)$$

Here, τ_1 is the maximum relaxation time for a network without bifunctional junctions ($n = 1$), given by eq 74. The expression for the maximum relaxation time τ_{max} given by eq 81 is similar to that obtained by Graessley,[12]

who set a different time scale. Graessley[12] assumed that frictional interactions along the strands might be localized at the junctions, so that each junction has an effective frictional coefficient

$$\zeta = \phi n \zeta_0/2 \tag{82}$$

Here, ζ_0 is the frictional coefficient of each monomer unit along the chain, and the primary relaxation time τ_0^G setting Graessley's time scale is

$$\tau_0^G = \frac{\zeta}{2K\phi} = \frac{n^2\zeta_0\langle r_1^2\rangle_0}{12k_BT} \tag{83}$$

where $K = 3k_BT/\langle r_n^2\rangle_0$ is the effective spring constant for chains between cross-links composed of n subchains, and $\langle r_1^2\rangle_0$ is the mean-square end-to-end distance ($\langle r_n^2\rangle_0 = n\langle r_1^2\rangle_0$) for a single subchain in the undeformed state. Taking into account bifunctional junctions gives us a more realistic description of the spectrum, especially at shorter times. The long-time end of the spectrum can be satisfactorily described by ignoring strand modes, as has been done by Graessley.[12] To calculate the relaxation spectrum for the network we made the following assumptions:

I. The network is an ideal, symmetrically grown infinite tree of functionality ϕ with no loops and dangling chains and with all chains and subchains of equal length. Peripheral junctions are anchored to fixed junctions, which do not fluctuate.

II. The chains are Gaussian and phantomlike.

III. The frictional coefficients ζ for bifunctional and multifunctional junctions are the same.

IV. The relaxation spectrum for elements of the network far removed from the fixed junctions can be separated from the rest of the spectrum.

Only assumption III can be relatively easily removed, as shown in Appendix C. The most controversial is assumption IV, which permits analytical solution of the problem. It might be difficult to compare our results with experimental data since real networks do not have the topology of an ideal, symmetrical tree. Dangling chains and loops, which exist in all real networks, might considerably change the relaxation spectrum. The polydispersity of chain lengths and the network's functionality might additionally influence the relaxation spectrum of the network. Entanglement effects that play an important role for real networks might also affect its relaxation spectrum.

In spite of the above qualifications, the results obtained do shed considerable light on the relaxation spectrum to be expected for a Gaussian network.

Acknowledgment. It is a pleasure to acknowledge the financial support provided by the National Science Foundation through Grants DMR 84-15082 for J.E.M. and DMR 85-15519 for H.L.F. (Polymers Program, Division of Materials Research) and to thank Professors Burak Erman, Bruce E. Eichinger, and William W. Graessley for discussions and very helpful comments.

Appendix A

We follow the standard method[6] of solving recurrence relations of this type. Instead of the coefficients A_k we introduce new coefficients

$$B_k = A_k/\sqrt{\phi - 1} \tag{A1}$$

so that

$$B_k = \frac{U_n(x) + (\phi - 2)U_{n-1}(x) - (\phi - 1)U_{n-2}(x)}{\sqrt{\phi - 1}} - \frac{1}{B_{k-1}} \tag{A2}$$

for $2 \le k \le J$.

We also make the substitution

$$\frac{U_n(x) + (\phi - 2)U_{n-1}(x) - (\phi - 1)U_{n-2}(x)}{\sqrt{\phi - 1}} = z + \frac{1}{z} \tag{A3}$$

Now we are looking for the solution of the recurrence relation given by eq A2 in the form

$$B_k = \frac{\alpha_0 + \alpha_1 z^2 + \alpha_2 z^4 + \ldots + \alpha_k z^{2k}}{z(\alpha_0 + \alpha_1 z^2 + \alpha_2 z^4 + \ldots + \alpha_{k-1} z^{2k-2})} \tag{A4}$$

where $\alpha_0, \alpha_1, \ldots, \alpha_k$ are z-independent unspecified coefficients. Substituting the above expression for B_k into

$$B_k + \frac{1}{B_{k-1}} = z + \frac{1}{z} \qquad 2 \le k \le J \tag{A5}$$

we find that all coefficients $\alpha_0, \alpha_1, \ldots, \alpha_k$ might be arbitrary with the only requirement

$$\alpha_k = \alpha_{k-1} \tag{A6}$$

Since eq A5 has to be satisfied for all $2 \le k \le J$, then

$$\alpha_1 = \alpha_2 = \alpha_3 = \ldots = \alpha_{k-1} = \alpha_k = 1 \tag{A7}$$

For simplicity, we set all these coefficients equal to 1. For $k = 1$ we have

$$B_1 = \frac{\alpha_0 + z^2}{\alpha_0 z} \tag{A8}$$

With the help of eqs A7 and A8, eq A4 might be written

$$B_k = \frac{B_1(z^k - z^{-k}) - (z^{k-1} - z^{-(k-1)})}{B_1(z^{k-1} - z^{-(k-1)}) - (z^{k-2} - z^{-(k-2)})} \tag{A9}$$

for $2 \le k \le J$. If we assume that $z + 1/z$ is real, then it follows[6] $|z| = 1$ or equivalently

$$z = e^{i\Psi} \tag{A10}$$

with

$$\cos\Psi = \frac{U_n(x) + (\phi - 2)U_{n-1}(x) - (\phi - 1)U_{n-2}(x)}{2\sqrt{\phi - 1}} \tag{A11}$$

Equation 38 for the eigenvalues becomes

$$B_k = \frac{B_1 \sin(k\Psi) - \sin[(k-1)\Psi]}{B_1 \sin[(k-1)\Psi] - \sin[(k-2)\Psi]} = 0 \tag{A12}$$

with

$$B_1 = \frac{U_n(x) + (\phi - 2)U_{n-1}(x)}{\sqrt{\phi - 1}} \tag{A13}$$

We obtain eq 41 by using the trigonometric representation and recursion formula for Chebyshev polynomials in eq A12 and the relation between A_k and B_k (eq A1). By direct checking of eq 41 for small trees, one might find that the equation is correct although it was derived with the simplifying assumption of the reality of $B_k + 1/B_{k-1}$.

Appendix B

Equation 43 can be written as

$$U_{k+1}(y) - U_k(y) + [\sqrt{\phi - 1}U_{n-2}(x) + 1]U_k(y) = 0 \quad \text{(B1)}$$

for $0 \le k \le J - 2$, with y and x given by eqs 42 and 21, respectively. Assuming that for large k the difference might be replaced by a differential, we have

$$\frac{dU_k(y)}{dk} + [\sqrt{\phi - 1}U_{n-2}(x) + 1]U_k(y) = 0 \quad \text{(B2)}$$

The solution of this differential equation is

$$U_k(y) = \exp\{-k[\sqrt{\phi - 1}U_{n-2}(x) + 1]\} \quad \text{(B3)}$$

If

$$\sqrt{\phi - 1}U_{n-2}(x) + 1 > 0 \quad \text{(B4)}$$

then in the limit $k \to \infty$, i.e., for tiers far removed from the surface, we have

$$U_k(y) = 0 \quad \text{(B5)}$$

which means

$$U_n\left(1 - \frac{\lambda}{2}\right) + (\phi - 2)U_{n-1}\left(1 - \frac{\lambda}{2}\right) - (\phi - 1)U_{n-2}\left(1 - \frac{\lambda}{2}\right) = 2\sqrt{\phi - 1}\cos\frac{\pi r}{k + 1} \quad \text{(B6)}$$

with $r = 1, 2, \ldots, k$.

For $n = 1$, eq B6 gives Graessley's result.[12] A different kind of argument supporting this derivation of eq B6 is given below. Equation A12 for the eigenvalues reads

$$B_1U_{k-1}(y) - U_{k-2}(y) = 0 \quad \text{(B7)}$$

with y given by eq 42. Here, B_1 is the value of B for the peripheral tier directly connected with fixed junctions. We assumed that matrix $\mathbf{A}_n$ given by eq 10 describes also the last tier; i.e., the functionality of the ϕ-functional junction in the last tier is preserved as shown in Figure 5a. Because of this B_1 is given by eq A13.

The relaxation spectrum from the elements of the network far removed from the boundary should be relatively weakly dependent on the structure of the anchoring of peripheral junctions to fixed junctions. For example, if peripheral junctions are anchored to single fixed junctions (the ϕ-functionality of peripheral junctions is not preserved) as shown in Figure 5b, then

$$B_1 = \frac{U_n(1 - \lambda/2)}{\sqrt{\phi - 1}} \quad \text{(B8)}$$

The assumption that the relaxation spectrum from the elements of the network infinitely far removed from fixed junctions is independent of the structure of anchoring of the network to fixed junctions implies the B_1 independence of eq B7 for the eigenvalues. If eq B7 is independent of B_1, then

$$U_{k-2}(y) = 0 \quad \text{(B9)}$$

for $k \to \infty$. We obtain the same result in the limit $k \to \infty$ if

$$B_1 = 2y = \frac{U_n(x) + (\phi - 2)U_{n-1}(x) - (\phi - 1)U_{n-2}(x)}{\sqrt{\phi - 1}} \quad \text{(B10)}$$

since then eq B7 becomes

$$U_k(y) = 0 \quad \text{(B11)}$$

The validity of our approximation might also be shown analytically for the case $\phi = 2$. For $\phi = 2$ the exact solution of the problem is

$$U_{kn}\left(1 - \frac{\lambda}{2}\right) = 0 \qquad 1 \le k \le J - 1 \quad \text{(B12)}$$

while the approximate solution (eq B5) is

$$U_{k-1}\left[T_n\left(1 - \frac{\lambda}{2}\right)\right] = \frac{1}{U_{n-1}\left(1 - \frac{\lambda}{2}\right)}U_{kn-1}\left(1 - \frac{\lambda}{2}\right) = 0 \quad \text{(B13)}$$

for $1 \le k \le J - 1$. In the limit $k \to \infty$, solutions of eqs B12 and B13 have the same functional form; specifically

$$\lambda_r = 2 - 2\cos\frac{\pi r}{nk} \quad \text{(B14)}$$

The equation for eigenvalues associated with the central tier (eq 50) is completely different from the equation for eigenvalues for other tiers (eq 43); nevertheless, it can be shown that both equations have similar asymptotic solutions for infinitely large networks.

Equation 50 has two branches of solutions:

$$U_k(y) + \left[\sqrt{\phi - 1}U_{n-1}(x) - \frac{1}{\sqrt{\phi - 1}}\right]U_{k-1}(y) - U_{n-1}(x)U_{k-2}(y) = 0 \quad \text{(B15)}$$

and

$$U_k(y) + \left[\sqrt{\phi - 1}U_{n-1}(x) + \frac{1}{\sqrt{\phi - 1}}\right]U_{k-1}(y) + U_{n-1}(x)U_{k-2}(y) = 0 \quad \text{(B16)}$$

with y given by eq 42 and x by eq 21. Assuming that for large k the differences might be replaced by differentials (as was done in deriving eq B2), we may write eqs B15 and B17 as second-order linear differential equations, with constant (k independent) coefficients, of the type

$$\frac{d^2U_k(y)}{dk^2} + \alpha(\phi,x)\frac{dU_k(y)}{dk} + \beta(\phi,x)U_k(y) = 0 \quad \text{(B17)}$$

Here, α and β are these constant coefficients dependent only on ϕ and x. Equation B17 resembles the equation of motion for a damped harmonic oscillator (with k corresponding to time); i.e., the asymptotic solution of eq B17 in the limit $k \to \infty$ (for infinitely large network) is

$$\lim_{k\to\infty} U_k(y) = 0 \quad \text{(B18)}$$

for $k = J$.

This means that the asymptotic solution for the central tier is the same as asymptotic solutions (eq B5) for other tiers, as expected since there is now no special reason for any extraordinary behavior of the central tier.

Appendix C

If the frictional coefficient ζ_m for the multifunctional junctions differs from the frictional coefficient ζ_2 for bifunctional ones, then eq 22 becomes

$$\det(\mathbf{A}_n - \lambda\mathbf{I}_n) = (\phi - \gamma\lambda)U_{n-1}(x) - U_{n-2}(x) \quad \text{(C1)}$$

where γ is the ratio of frictional coefficients

$$\gamma = \zeta_m/\zeta_2 \quad \text{(C2)}$$

and x is given by eq 21.

Instead of eqs 39 and 40 we have

$$A_1 = \gamma U_n(x) + (\phi - 2\gamma)U_{n-1}(x) + (\gamma - 1)U_{n-2}(x) \quad \text{(C3)}$$

and

$$A_k = \gamma U_n(x) + (\phi - 2\gamma)U_{n-1}(x) - (\phi - \gamma)U_{n-2}(x) - \frac{\phi - 1}{A_{k-1}(x)} = 0 \quad \text{(C4)}$$

The solution of this recurrence relation is given also by eq 41 but with y differently defined:

$$y = \frac{\gamma U_n(x) + (\phi - 2\gamma)U_{n-1}(x) - (\phi - \gamma)U_{n-2}(x)}{2\sqrt{\phi - 1}} \quad \text{(C5)}$$

It can be checked that $y(1)$ does not depend on γ and is given by eq 76, so that even for different frictional coefficients, there is always a finite maximum relaxation time.

Since

$$y'(1) = \frac{n}{2\sqrt{\phi - 1}}(n\phi - \phi + 2\gamma) \quad \text{(C6)}$$

the approximate maximum relaxation time becomes

$$\tau_{max}^{appr} = \tau_0 \frac{n(n\phi - \phi + 2\gamma)}{2(\phi - 2\sqrt{\phi - 1})} \quad \text{(C7)}$$

Here, the primary relaxation time τ_0 of a single unattached subchain is

$$\tau_0 = \zeta_2/K \quad \text{(C8)}$$

where the spring constant K is given by eq 3.

For ζ_m greater than ζ_2 ($\gamma > 1$), the maximum relaxation time increases in comparison with the previously studied case of all beads having the same friction coefficient.

References and Notes

(1) Rouse, P. E. *J. Chem. Phys.* **1953**, *21*, 1272.
(2) Doi, M.; Edwards, S. F. The *Theory of Polymer Dynamics*; Oxford University Press: Oxford, 1986.
(3) Zimm, B. H. *J. Chem. Phys.* **1956**, *24*, 269.
(4) Chompff, A. J.; Duiser, J. A. *J. Chem. Phys.* **1966**, *45*, 1505.
(5) Chompff, A. J.; Prins, W. *J. Chem. Phys.* **1968**, *48*, 235.
(6) Chompff, A. J. *J. Chem. Phys.* **1970**, *53*, 1566.
(7) Chompff, A. J. *J. Chem. Phys.* **1970**, *53*, 1577.
(8) Jernigan, R. L. In *Dielectric Properties of Polymers*; Karasz, F. E., Ed.; Plenum Press: New York, 1972; p 99.
(9) Bahar, I.; Erman, B. *Macromolecules* **1987**, *20*, 1368.
(10) Erman, B. "Dynamic Rotational Isomeric State Model", preprint.
(11) Doi, M. *Polym. J.* **1974**, *6*, 108.
(12) Graessley, W. W. *Macromolecules* **1980**, *13*, 372.
(13) Rubin, R. J.; Zwanzig, R. *J. Math. Phys.* **1961**, *2*, 861.
(14) Martin, J. E.; Eichinger, B. E. *Macromolecules* **1980**, *13*, 626.
(15) Eichinger, B. E.; Martin, J. E. *J. Polym. Sci., Polym. Lett. Ed.* **1979**, *17*, 209.
(16) Eichinger, B. E. *Macromolecules* **1972**, *5*, 496.
(17) McKay, B. D. Mathematics Research Report No. 9, University of Melbourne, 1979.
(18) Ronca, G. *J. Chem. Phys.* **1980**, *72*, 48.
(19) Kloczkowski, A.; Mark, J. E.; Erman, B. *Macromolecules* **1989**, *22*, 1423.
(20) Abramowitz, M.; Stegun, I. E. *Handbook of Mathematical Functions*; National Bureau of Standards: Washington, DC, 1964.
(21) Rivlin, T. J. *The Chebyshev Polynomials*; Wiley: New York, 1974.